

1 **Carbonation of alkaline paper mill waste to reduce CO₂ greenhouse gas**
2 **emissions into the atmosphere**

3

4 R. Pérez-López^{*,a,b}, G. Montes-Hernandez^a, J.M. Nieto^b, F. Renard^{c,d}, L. Charlet^a

5

6 ^a LGIT, CNRS-OSUG-UJF, Université Joseph Fourier, Grenoble I, Maison des Géosciences, BP 53,
7 38041 Grenoble Cedex, France

8 ^b Department of Geology, University of Huelva, Campus 'El Carmen', 21071, Huelva, Spain

9 ^c LGCA, CNRS-OSUG-UJF, Université Joseph Fourier, Grenoble I, Maison des Géosciences, BP 53,
10 38041 Grenoble Cedex, France

11 ^d Physics of Geological Processes, University of Oslo, Norway

12

13

14 To be submitted to Applied Geochemistry on December 18th, 2007

15

* Corresponding author. Tel.: +34-95-921-9826; fax: +34-95-921-9810

E-mail address: rafaelperez@dgeo.uhu.es (R. Pérez-López)

16 **Abstract**

17

18 The global warming of Earth's near-surface, air and oceans in recent decades is a direct
19 consequence of anthropogenic emission of greenhouse gases into the atmosphere such as CO₂,
20 CH₄, N₂O and CFCs. The CO₂ emissions contribute approximately 60% to this climate change.
21 This study investigates experimentally the aqueous carbonation mechanisms of an alkaline paper
22 mill waste containing about 55 wt% of portlandite (Ca(OH)₂) as a possible mineralogical carbon
23 dioxide sequestration process. The overall carbonation reaction includes the following steps: (1)
24 Ca release from the portlandite dissolution, (2) CO₂ dissolution in water and (3) calcium
25 carbonate precipitation. This CO₂ sequestration mechanism was supported by geochemical
26 modelling of final solutions using PHREEQC software, and observations of scanning electron
27 microscope and X-ray diffraction of final reaction products. According to our experimental
28 protocol, the system proposed would favour the total capture of approx. 218 kg of CO₂ into stable
29 calcite per every ton of paper waste, independently of initial CO₂ pressure. The final product
30 from carbonation process is a calcite (ca. 100 wt%)-water dispersion. Indeed, the total captured
31 CO₂ mineralized as calcite could easily be stored in soils or in the ocean without any significant
32 environmental negative impact. This result demonstrates the possibility to use the alkaline liquid-
33 solid waste for CO₂ mitigation and reduction of greenhouse effect gases into the atmosphere.

34

35 **Keywords:** *Portlandite; Paper waste; Aqueous carbonation; Mineral trapping of CO₂; Calcite*

36

37 **1. Introduction**

38

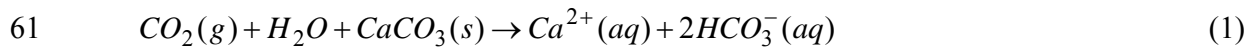
39 Coal caused the first industrial revolution that transformed the agrarian societies. Electricity
40 allowed the formation of great urban centres. The advance of the industrialized societies has
41 taken place in exchange for the unconditional burning of fossil fuels. This has caused an increase
42 of the CO₂ concentration in the atmosphere from 280 ppm in the pre-industrial revolution to 379
43 ppm in 2005, rising faster in the last 10 years (average 1995-2005: 1.9 ppm yr⁻¹) (IPCC, 2007a).

44 The temperature of Earth's near-surface, air and oceans is basically controlled by the capacity
45 of the atmosphere to reflect, adsorb and emit the solar energy. However, the continuous
46 emissions of CO₂ into the atmosphere (26.4 ± 1.1 Gt CO₂ yr⁻¹ for 2000-2005) have altered this
47 natural equilibrium and have led to the increase of the greenhouse effect and the consequent
48 climatic change. The global surface average temperature will increase 2-4.5 °C when the
49 atmospheric CO₂ concentration doubles the pre-industrial revolution concentration (IPCC,
50 2007a). These alterations are leading to stress on drinking water availability, species extinction,
51 melting of ice sheets and coastal flooding (IPCC, 2007b).

52 The energy production system is currently profitable, thus any modification is unviable since
53 it could produce huge imbalances in the global economy. An alternative to reduce the CO₂
54 emission is the retention of carbon dioxide in natural reservoirs. Three possibilities for
55 sequestration of carbon dioxide are currently being studied: aqueous carbon sequestration,
56 geological carbon sequestration and mineralogical carbon sequestration.

57 Aqueous carbon sequestration involves the CO₂ dissolution into water to produce a carbonic
58 acid solution, which later is neutralized and equilibrated with limestone as shown by the
59 following reaction (Rau et al., 2007):

60



62

63 The dissolved calcium bicarbonate produced is then released and diluted in the ocean where
64 these ions are already present abundantly in seawater. Moreover, this process is geochemically
65 comparable to the natural mechanism of CO₂ mitigation by continental and marine carbonate
66 weathering, but over many millennia time scales (Murray and Wilson, 1997).

67 Geological carbon sequestration consists of capturing gaseous CO₂ from emission sources
68 and injecting it in terrestrial reservoirs, such as saline aquifers, depleted oil and gas fields or deep
69 coal seams (Bachu, 2000, 2002; Bachu and Adams, 2003; Friedmann, 2007). The main scientific
70 concerns involving the geological carbon sequestration applicability are the high pressure and
71 temperature variations caused by the large CO₂ accumulation on the reservoirs. These
72 thermodynamic variations could exert forces that diminish the reservoir confinement due to the
73 formation of cracks and faults either in reservoir itself, or in the cap rocks. Moreover, the CO₂
74 dissolution into the pore water and the consecutive carbonic acid formation can result in the rapid
75 dissolution of several minerals (mainly carbonate, oxides and hydroxide minerals) affecting the
76 long-term confinement properties of the reservoirs (Kharaka et al., 2006).

77 In terrestrial reservoirs, the CO₂ pressure can decrease in the long term as a consequence of a
78 mineralogical carbon sequestration or mineral trapping. The stored CO₂ may transform to stable
79 carbonate minerals by reactions with aqueous ions (mainly calcium, magnesium and iron)
80 resulting from silicate weathering (Gunter et al., 2000; Kaszuba et al., 2003, 2005; Giammar et
81 al., 2005; Bénézech et al., 2007). Although this mechanism favours the permanent CO₂
82 sequestration, it is expected to be slow in geological formation (hundreds of years) due to the
83 slow kinetics of silicate mineral dissolution and carbonate mineral precipitation. However, the

84 mineralogical carbon sequestration could contribute significantly to CO₂ sequestration in the
85 proximity of the emission source, without the need of storing the gas into a geological reservoir.
86 Some authors proposed the use of mineralogical carbon sequestration in controlled reactors as a
87 viable approach to reduce CO₂ emissions into the atmosphere using either: (1) industrial by-
88 products such as coal combustion fly-ash (Montes-Hernandez et al. 2007a), coal combustion fly-
89 ash plus brine solution from gas production (Soong et al., 2006) or municipal solid waste bottom-
90 ash (Rendek et al., 2006); or (2) primary minerals such as serpentine/olivine (Maroto-Valer et al.,
91 2005) or wollastonite (Huijgen et al., 2006). These materials act as calcium and magnesium
92 source favouring the CO₂ retention by carbonate precipitation.

93 Montes-Hernandez et al. (2007b) proposed an experimental method to synthesize fine
94 particles of calcite by means of aqueous carbonation of pure portlandite at high pressure of CO₂
95 (initial P_{CO₂}=55 bar) and moderate and high temperature (30 and 90 °C). This aqueous
96 carbonation process implies dissolution of CO₂ into water and the consequent calcite
97 precipitation. This method also has important ecological implications for mineral carbon
98 sequestration. However, the use of pure portlandite and other primary minerals may suppose a
99 high economic and environmental cost as these are typically resources and not residues.

100 In the cellulose pulp production for paper manufacture, the dominant process involves
101 cooking woodchips in high concentrations of sodium hydroxide and sodium sulphide for 2-4 h at
102 170 °C. This process, known as kraft pulping, favours the lignin dissolution and the separation of
103 the cellulose fibers that are recovered by means of sieving. The residual liquids or black liquor
104 containing the most of the dissolved lignin are transformed to white liquor and reused in the
105 cooking stage. This transformation is carried out by both combustion in a boiler and causticizing
106 with lime and implies the production of several types of portlandite-rich solid wastes with
107 alkaline nature known generically as alkaline paper mill wastes.

108 In some pulp and paper industries, the alkaline by-products are usually sold for the cement
109 manufacture and as alkaline amendment for agricultural soils. Nevertheless, their recycling is
110 limited by the presence of chloride and metals, and in numerous occasions must be stored near
111 the industrial facilities. A few investigations focused on the reusability of these wastes have been
112 reported in the literature, and the existing ones are based on their application for the
113 neutralization of acid mine drainages (Bellaloui et al., 1999). The main aim of this paper is to
114 show the efficiency of the utilization of these wastes as a calcium source for aqueous
115 carbonation, calcite precipitation and mineralogical CO₂ sequestration. From the sustainable
116 development point of view, the treatment proposed is especially attractive because a low-cost
117 residue is used to reduce the emissions of greenhouse gasses into the atmosphere.

118

119

120 **2. Materials and methods**

121

122 *2.1. Alkaline paper mill waste*

123

124 The alkaline paper waste used in the present study was collected from a cellulose pulp factory
125 (ENCE) located in Huelva, south-western Spain. This by-product, so-called calcium mud, is the
126 waste of the calcination or conversion of calcium carbonate to lime for the causticizing of the
127 black liquor. Calcium mud was selected since it presents a higher Ca content than the remaining
128 alkaline paper wastes.

129 The particle size of paper mill waste ranges from 1 to 100 μm with a median size of 15 μm,
130 as determined by laser diffraction. This waste is made up of portlandite (Ca(OH)₂; 55 wt%),
131 calcite (CaCO₃; 33 wt%) and hydroxyapatite (Ca₁₀(PO₄)₆(OH)₂; 12 wt%). The portlandite

132 particles present a laminar-pseudo-hexagonal habit, as observed by scanning electron microscopy
133 equipped with an energy dispersive system (SEM-EDS, JEOL JSM-5410 instrument) (Fig. 1).
134 The chemical composition analyzed with X-ray fluorescence (XRF, BRUKER PIONEER
135 instrument) shows high content of Ca (83.2 wt% CaO), C (10.3 wt% CO₂), P (2.4 wt% P₂O₅), S
136 (2 wt% SO₃), Na (0.88 wt% Na₂O), Mg (0.35 wt% MgO), Si (0.34 wt% SiO₂), Al (0.17 wt%
137 Al₂O₃) and K (0.13 wt% K₂O), and minor amounts of Cl (590 ppm), Fe (137 ppm), Ni (130
138 ppm), Sr (114 ppm) and Cu (108 ppm). The water content determined by drying at 105 °C until
139 constant weight was about 21 wt%. The presence of high concentrations of portlandite in paper
140 mill waste accounts for the high alkalinity and potential for carbon dioxide sequestration as
141 discussed below.

143 2.2. CO₂ sequestration experiments

144
145 The CO₂ sequestration experiments were conducted in a 2 L (total volume) closed titanium-
146 lined pressure reactor (Parr Instrument Co., USA, Model 4843) equipped with a heating jacket
147 (Fig. 2). In each experiment, the autoclave was charged with approximately 1L of Millipore MQ
148 water (18.2 MΩ) and 20 g of paper mill waste. The waste particles were immediately dispersed
149 with mechanical agitation (450 rpm) and the dispersion heated to 30 or 60 °C. When the
150 temperature was reached, 10, 20, 30 or 40 bar of CO₂ (provided by Linde Gas S.A.) was injected
151 into the reactor by opening a valve and adjusting the pressure to the desired one, and the reaction
152 was commenced. This initial pressure of CO₂ was equal to the total initial pressure in the system.
153 A summary of the experiments carried out and the initial experimental conditions is shown in
154 Table 1. A long-term experiment (48 hours) at 30 bar of initial pressure of CO₂ allowed us to

155 both optimize the experimental duration of the remaining experiments at 2 hours and study the
 156 kinetic evolution of the carbonation process.

157 The global pressure drop in the system, $P_{global_pressure-drop}$, is a consequence of both the
 158 dissolution-dissociation of CO_2 in the solution and aqueous carbonation process of $Ca(OH)_2$. In
 159 order to calculate the pressure drop only produced by the carbonation process
 160 ($P_{carbonation_pressure-drop}$), two independent but complementary experiments were proposed for
 161 each experiment: (1) to measure the pressure drop related to the dissolution-dissociation of CO_2
 162 into pure water ($P_{water_pressure-drop}$), and (2) to measure the pressure drop related to the
 163 dissolution-dissociation of CO_2 in a Ca-rich solution ($P_{Ca-rich_pressure-drop}$). In this second
 164 experiment, a concentration of 1 g L^{-1} of calcium was chosen, that represented the average
 165 concentration after paper waste dispersion in water. These two experiments demonstrated that the
 166 Ca-concentration ($0\text{-}1\text{g L}^{-1}$) has no measurable effect on the dissolution-dissociation of CO_2 since
 167 the monitored pressure drop in pure water ($P_{water_pressure-drop}$) was equivalent to the monitored
 168 pressure drop in presence of Ca ($P_{Ca-rich_pressure-drop}$). Consequently, the pressure drop produced
 169 by the carbonation process of $Ca(OH)_2$ was calculated by a simple pressure balance:

170

$$171 \quad P_{carbonation_pressure-drop} = P_{global_pressure-drop} - P_{water_pressure-drop} \quad (2)$$

172

173 Under isothermal conditions, $P_{global_pressure-drop}$ and $P_{water_pressure-drop}$ are proportional to the
 174 initial CO_2 pressure.

175 At the end of the experiment, the reactor was removed from the heating system and was
 176 immersed in cold water. The reaction cell was depressurized during the cooling water period at

177 25 °C (about 15 minutes). Subsequently, the reactor was disassembled and the supernatant was
178 separated from the solid product by centrifugation at 12,000 rpm for 30 minutes. Finally, the
179 solid product was dried directly in the centrifugation flasks for 48 h at 65 °C. The supernatant
180 solutions were filtered through a 0.2- μm Teflon filter. Adsorption on the filter and filter holder
181 was considered negligible. The filtered solutions were immediately acidified for measurement of
182 [Ca], [Ni], [Zn], [Cu] and [Sr] by Inductively Coupled Plasma Atomic Emission Spectrometry
183 (ICP-AES).

184

185 *2.3. Characterization of solid phase*

186

187 The mineralogical characterization of the starting material and solid products was carried out
188 by X-ray diffraction (XRD, powder method) using a D501 SIEMENS diffractometer. Working
189 conditions were $\text{CoK}\alpha$ monochromatic radiation ($\lambda=1.7902 \text{ \AA}$), 37.5 mA and 40 kV. The
190 experimental measurement parameters were 12 s counting time per $0.02^\circ 2\theta$ step in the $5\text{-}80^\circ 2\theta$
191 range. The detection is performed by a Kevex Si(Li) detector. Morphological analyses of solid
192 products were also characterized by means of SEM-EDS.

193 Solution saturation indexes with respect to solid phases ($\text{SI}=\log(\text{IAP}/\text{K}_s)$, where SI is the
194 saturation index, IAP is the ion activity product and K_s is the solid solubility product) and
195 aqueous speciation of the leachates were calculated using the equilibrium geochemical
196 speciation/mass transfer model PHREEQC (Parkhurst and Appelo, 2005) and the database of the
197 speciation model MINTEQ. Zero, negative or positive SI values indicate that the solutions are
198 saturated, undersaturated and supersaturated, respectively, with respect to a solid phase.

199

200

201 **3. Results and discussion**

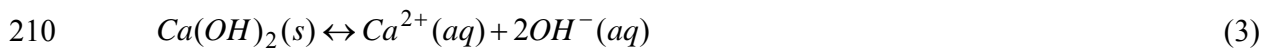
202

203 *3.1. Reaction mechanisms of CO₂ sequestration*

204

205 In an aqueous system, the water-CO₂-paper waste interaction would suppose the carbonation
 206 of portlandite (Ca(OH)₂; 55 wt%) according to well-known reactions (3-7) described in numerous
 207 works (e.g., Juvekar and Sharma, 1973; Shih et al., 1999; Beruto and Botter, 2000). On one hand,
 208 the calcium hydroxide is dissociated and increases the pH up to values around 12 (Eq. 3):

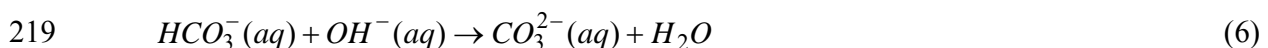
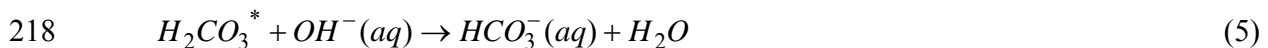
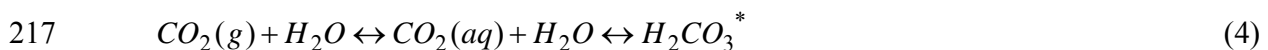
209



211

212 On the other hand, the gaseous CO₂ is dissolved into the solution and reacts with the water to
 213 form carbonic acid (Eq. 4). Once equilibrium is established between the gaseous CO₂ and H₂CO₃,
 214 the carbonic acid further dissociates into bicarbonate and carbonate ions (Eqs. 5 and 6). At
 215 alkaline pH, the carbonate ion (CO₃²⁻) is the dominant species occurring in solution.

216



220

221 The presence of CO₃²⁻ anions together with high Ca concentrations from the portlandite
 222 dissolution favours the supersaturation, and hence, the precipitation of calcium carbonate (Eq. 7):

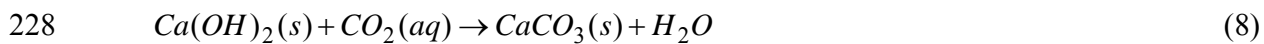
223



225

226 The overall reaction for the process can be written as:

227



229

230 The thermodynamic calculations and the mineralogical characterization of solid products
231 after experiments suggest that this simple reaction mechanism explains the CO₂ sequestration by
232 paper mill waste. After the reaction, PHREEQC code indicates that the solutions are
233 supersaturated with respect to calcium carbonate. Saturation indexes of calcite are in the range
234 1.13-1.71 (Table 1). Comparison of X-ray diffraction spectra of the starting material and the solid
235 product demonstrates that the portlandite contained in the starting material is totally carbonated
236 and transformed to calcite (Fig. 3). The precipitated calcite is characterized by micrometric
237 agglomerates of rhombohedral-crystals (Fig. 4). Both pre-existing calcite and hydroxyapatite in
238 the starting material do not intervene in the CO₂ sequestration process.

239 One possible disadvantage of using paper mill waste is that this waste contains initially some
240 toxic elements such as Ni, Zn, Cu and Sr that may be released in solution. However, the
241 carbonation process also favoured the co-precipitation and/or incorporation of the dissolved
242 impurities into the calcite crystal lattice. In fact, the Ni, Zn and Cu concentrations were below
243 detection limit ($< 6 \mu\text{g L}^{-1}$). Strontium was the only trace element detected by ICP-AES ($[\text{Sr}] \approx$
244 0.25 mg L^{-1}) in the solution. Nevertheless, the Sr concentrations are lower than the ones that

245 should have a pre-potable water for human consumption according to the established
 246 requirements by World Health Organisation (4 mg L⁻¹).

247 In summary, the final product from carbonation process is a solid containing ca. 100 wt% of
 248 calcite, as occurs with the experiments from Montes-Hernandez et al. (2007b), but using a low-
 249 cost portlandite-rich waste instead of pure portlandite. Moreover, taking into account that the
 250 paper mill waste does not favour the liberation of toxic metallic ions at the CO₂ sequestration
 251 experiments, the final calcite-water dispersion could be used as reagent for a further aqueous
 252 carbon sequestration (see Introduction, Eq. 1). Hence, the final result of these experiments would
 253 allow us to continue sequestering CO₂ and the total amount of captured CO₂ could be poured
 254 either directly into the sea (not contribute with trace elements), being even beneficial for marine
 255 biota (Rau et al., 2007) or into soils.

256

257 3.2. Amount of sequestered CO₂

258

259 A simplified method was developed to estimate the quantity of CO₂ sequestered by carbonate
 260 precipitation. This method was partially described in the section 2.2. Herein, the pressure drop
 261 produced by the carbonation process of Ca(OH)₂ (Eq. 8) in the system was calculated by a simple
 262 pressure balance (Eq. 2). Knowing the pressure drop values in each experiment (Table 1), the
 263 amount of CO₂ consumed by calcite precipitation ($n_{carbonation_CO_2,real}$ in mol) could be calculated
 264 using the ideal gas law:

265

$$266 \quad n_{carbonation_CO_2,real} = \frac{P_{carbonation_pressure-drop}V}{RT} \quad (9)$$

267

268 where V is the reactor volume occupied with gas (1 L), T is the reaction temperature (≈ 303 °K)
 269 and R is the gas constant (0.08314472 L bar K⁻¹ mol⁻¹).

270 In experiments at 30 °C and 2 h of experimental duration, the pressure drop by portlandite
 271 carbonation was around 2.5 bar, independently of initial CO₂ pressure (Fig. 5a). Although the
 272 results of the long-term experiment (48 h, 30 bar and 30 °C) show that the equilibrium is obtained
 273 after about 5 hours of solid-fluid interaction, the maximum pressure drop by carbonation is
 274 already reached at 2 hours of experiment (Fig. 5b), and thus the experimental duration of the
 275 remaining experiments was correctly optimized. According to Eq. 9, the real amount consumed
 276 by carbonation was of 0.09923 mol of CO₂.

277 The theoretical amount of CO₂ ($n_{carbonation_CO_2,theoretical}$) that should be sequestered by
 278 carbonation process (i.e., if all calcium is carbonated) could be calculated based on both the
 279 stoichiometry of reaction (8) and the quantity of portlandite contained into the paper mill waste
 280 (55 wt%):

$$282 \quad n_{carbonation_CO_2,theoretical} = \frac{w_{Ca(OH)_2}}{M_{Ca(OH)_2}} \quad (10)$$

283
 284 where $M_{Ca(OH)_2}$ is the molar mass of Ca(OH)₂ (74.093 g mol⁻¹) and $w_{Ca(OH)_2}$ is the starting
 285 mass of Ca(OH)₂ in the reactor (8.69 g) which was calculated as follows:

$$287 \quad w_{Ca(OH)_2} = m_{paper_waste} \times \left(\frac{\% \text{ portlandite}}{100} \right) \times \left(1 - \frac{\% \text{ water_content}}{100} \right) \quad (11)$$

288

289 where m_{paper_waste} is the mass of paper mill waste used in the experiments (20 g), $\%_{portlandite}$ is
290 the percentage of portlandite in the waste (55 wt%) and $\%_{water_content}$ is the water content
291 percentage in the waste (21 wt%). The theoretical amount of CO₂ that should be sequestered is
292 0.11729 mol. This supposes a carbonation efficiency (CE) of 85% at 30 °C according to:

293

$$294 \quad CE = \frac{n_{carbonation_CO_2,real}}{n_{carbonation_CO_2,theoretical}} \times 100 \quad (12)$$

295

296 In the experiment at high temperature (60 °C, 30 bar), the pressure drop by carbonation is
297 slightly superior (3 bar), albeit the sequestered amount of CO₂ and the carbonation efficiency are
298 very similar since this process depends inversely on the reaction temperature (Eq. 9).

299 Theoretically, the extrapolation of this experiment to real industrial scale would suppose a
300 maximum CO₂ sequestration capacity of 258.54 kg of CO₂ per every ton of paper mill waste
301 containing 55 wt% of portlandite. However, with our experimental protocol, 218.37 kg of CO₂
302 per every ton of paper mill waste could be successfully sequestered into stable calcite. Obviously,
303 this is an attractive result concerning the mineral trapping of CO₂.

304

305 *3.3. Kinetic modelling of sequestered CO₂*

306

307 The monitoring of the pressure drop for any controlled system under ideal gas conditions
308 allows the kinetic modelling of sequestered CO₂ after gas injection in a solid-liquid system (paper
309 mill waste-water dispersion for this study). This can be done using a simple correlation function,

310 $n_{total_CO_2} = f(t)$, where $n_{total_CO_2}$ is the total mol quantity of sequestered CO₂ in the paper
 311 waste-water dispersion and t is the time after gas injection.

312 Several kinetic models including first-order, pseudo-first-order, second-order, pseudo-second-
 313 order, parabolic diffusion and power function kinetic expressions are reported in the literature for
 314 fitting the kinetic experimental or calculated data of solid-fluid interaction processes (e.g.
 315 Lagergren, 1898; Ho and Mckay, 1999). For this study, the kinetic modelling concerns the total
 316 sequestered quantity of CO₂ in a paper mill waste-water dispersion, i.e. the CO₂ dissolution-
 317 dissociation in water, possibly the CO₂ adsorption on the paper waste and, sequestered CO₂ by
 318 carbonation process. For this case, the best fit (attested by a correlation factor close to 1) of the
 319 experimental-calculated data was achieved when using a pseudo-second-order kinetic model
 320 according to the following expression:

$$322 \quad \frac{dn_{total_CO_2,t}}{dt} = k_s (n_{total_CO_2,max} - n_{total_CO_2,t})^2 \quad (13)$$

323
 324 where k_s is the rate constant of sequestered CO₂ [mol⁻¹ s⁻¹] for a given initial pressure of CO₂ in
 325 the system, $n_{total_CO_2,max}$ is the maximum sequestered quantity of carbon dioxide at equilibrium
 326 [mol], $n_{total_CO_2,t}$ is the sequestered quantity of carbon dioxide at any time, t , [mol].

327 The integrated form of Eq. 13 for the boundary conditions $t = 0$ to $t = t$ and $n_{total_CO_2,t} = 0$
 328 to $n_{total_CO_2,t} = n_{total_CO_2,t}$ is represented by a hyperbolic equation (Eq. 14):

329

330
$$n_{total_CO_2,t} = \frac{n_{total_CO_2,max} \times t}{\left(\frac{1}{k_s \times n_{total_CO_2,max}} \right) + t} \quad (14)$$

331
 332 In order to simplify the fitting of experimental-calculated data, we have defined the constant
 333 $t_{1/2} = 1/k_s \times n_{total_CO_2,max}$. Physically, $t_{1/2}$ represents the time after which half of the maximum
 334 sequestered quantity of carbon dioxide was reached and is called “half-sequestered CO₂ time”. It
 335 can be used to calculate the initial rate of sequestered CO₂, $v_{0,s}$, [mol s⁻¹] (Eq. 15):

336
 337
$$v_{0,s} = \frac{n_{total_CO_2,max}}{t_{1/2}} = k_s (n_{total_CO_2,max})^2 \quad (15)$$

338
 339 The fitting of the experimental-calculated kinetic curve at 30 bar and 30 °C ($n_{total_CO_2,t}$ vs.
 340 t) using Eq. 14 is shown in Figure 6. The parameters $t_{1/2}$ and $n_{total_CO_2,max}$ were estimated by
 341 applying non-linear regression using the least squares method. The initial rate of sequestered CO₂
 342 was calculated using the Eq. 15 ($v_{0,s} = 3.3 \times 10^{-4}$ mol s⁻¹) at 30 °C. This value indicates that the
 343 mass transfer of compressed CO₂ in contact with solid-water dispersion is higher than CO₂
 344 transfer at atmospheric conditions or at low pressure (Akanksha et al., 2007; Haubrock et al.,
 345 2007).

346

347

348 **4. Remarks and conclusions**

349

350 In search of the most effective technique to reduce the point CO₂ emissions into the
351 atmosphere, the aqueous carbonation of alkaline paper mill waste (approx. 55 wt% in portlandite)
352 could fulfil all necessary expectations for the following reasons:

353

354 1. The CO₂ sequestration is mainly produced by the portlandite dissociation, CO₂ dissolution
355 and calcite precipitation, as shown by means of XRD and SEM-EDS techniques, and
356 thermodynamic calculations with PHREEQC. According to our estimations, the system
357 proposed in this study would favour the mineralogical sequestration of approx. 218.37 kg
358 of CO₂ into stable calcite per every ton of paper waste. The amount sequestered by
359 carbonation is independent of both temperature (30 or 60 °C) and initial pressure of CO₂
360 injected in the system (10, 20, 30 or 40 bar).

361 2. The independence of temperature and pressure in the sequestration efficiency, probably
362 owing to that the reaction between portlandite and CO₂ is extremely fast, could reduce the
363 costs for the process in a industrial scale since: (1) additional energy is not required for the
364 excessive increasing of both parameters and (2) the system does not need special materials
365 for reactors design.

366 3. The capacity of mineral CO₂ sequestration of alkaline paper mill waste is much higher than
367 those in other materials reported in the literature. As a comparison, the municipal solid
368 waste bottom-ash could sequester 23.08 kg of CO₂ per ton (Rendek et al., 2006) and coal
369 combustion fly-ash 26.19 kg of CO₂ per ton (Montes-Hernandez et al. 2007a), that is, both
370 wastes present a sequestration capacity ca. 10 times lower than paper wastes. Wollastonite
371 presents a sequestration capacity very similar, i.e. 329 kg of CO₂ per ton (Huijgen et al.,
372 2006); however, this primary mineral is not a residue.

- 373 4. The result from carbonation process is a free-metal solution in contact with a solid
374 containing practically 100 wt% of calcite. This final product could be used as reagent for a
375 further aqueous carbon sequestration. The result of this additional CO₂ sequestration may
376 be stored in the ocean where it would add minimally to the large, benign pool of these ions
377 already present in seawater.
- 378 5. The generation of a solid product containing ca. 100% calcite also revalues the original
379 waste since this mineral is amply used in rubber, plastic, printing ink, paper making dope,
380 oil point, toothpaste, cosmetics and food industries (Chan et al., 2002; Kugge and Daicic et
381 al., 2004).
- 382 6. The utilization of other wastes to sequester CO₂ would result in the production of calcite in
383 a matrix of silicate minerals that would continue constituting a waste with low application.
384 In addition, these final products could be neither used for a further aqueous carbon
385 sequestration nor stored in soils or in the ocean.
- 386 7. The carbonation is an exothermic process for portlandite (Montes-Hernandez et al., 2007b),
387 which potentially reduces the overall energy consumption and costs of carbon
388 sequestration.

389

390 *Acknowledgements.* The authors wish to express their gratitude to ENCE S.A. (San Juan del
391 Puerto factory, Huelva) for samples of paper waste, the information offered and their support.
392 They are also grateful to the Agence Nationale pour la Recherche (ANR, project GeoCarbone-
393 CARBONATATION) and the Centre National pour la Recherche Scientifique (CNRS), for
394 providing a financial support for this work. Delphine Tisserand and Nicolas Geoffroy are thanked
395 for their technical assistance.

396

397 **References**

- 398
- 399 Akanksha, Pant, K.K., Srivastava, V.K., 2007. Mass transport correlation for CO₂ absorption in
400 aqueous monoethanolamine in a continuous film contactor. *Chem. Eng. Process.*
401 doi:10.1016/j.cep.2007.02.008.
- 402 Bachu, S., 2000. Sequestration of CO₂ in geological media: criteria and approach for site
403 selection in response to climate change. *Energy Convers. Manage.* 41, 953-970.
- 404 Bachu, S., 2002. Sequestration of CO₂ in geological media in response to climate change: road
405 map for site selection using the transform of the geological space into the CO₂ phase space.
406 *Energy Convers. Manage.* 43, 87-102.
- 407 Bachu, S., Adams, J.J., 2003. Sequestration of CO₂ in geological media in response to climate
408 change: capacity of deep saline aquifers to sequester CO₂ in solution. *Energy Convers.*
409 *Manage.* 44, 3151-3175.
- 410 Bellaloui, A., Chtaini, A., Ballivy, G., Narasiah, S., 1999. Laboratory investigation of the control
411 of acid mine drainage using alkaline paper mill waste. *Water Air Soil Poll.* 111, 57-73.
- 412 Bénézech, P., Palmer, D.A., Anovitz, L.M., Horita, J., 2007. Dawsonite synthesis and
413 reevaluation of its thermodynamic properties from solubility measurements: implications
414 for mineral trapping of CO₂. *Geochim. Cosmochim. Acta* 71, 4438-4455.
- 415 Beruto, D.T., Botter, R., 2000. Liquid-like H₂O adsorption layers to catalyze the Ca(OH)₂/CO₂
416 solid-gas reaction and to form a non-protective solid product layer at 20°C. *J. Eur. Ceram.*
417 *Soc.* 20, 497-503.
- 418 Chan, C.M., Wu, J.S., Li, J.X., Cheung, Y.K., 2002. Polypropylene/calcium carbonate
419 nanocomposites. *Polymer* 43, 2981-2992.
- 420 Friedmann, S.J., 2007. Geological Carbon Dioxide Sequestration. *Elements* 3, 179-184.

- 421 Giammar, D.E., Bruant, R.G., Peters, C.A., 2005. Forsterite dissolution and magnesite
422 precipitation at conditions relevant for deep saline aquifer storage and sequestration of
423 carbon dioxide. *Chem. Geol.* 217, 257-276.
- 424 Gunter, W.D., Perkins, E.H., Hutcheon, I., 2000. Aquifer disposal of acid gases: modeling of
425 water-rock reactions for trapping of acid wastes. *Appl. Geochem.* 15, 1085-1095.
- 426 Haubrock, J., Hogendoorn, J.A., Versteeg, G. F., 2007. The applicability of activities in kinetic
427 expressions: A more fundamental approach to represent the kinetics of the system CO₂-OH⁻
428 -salt in terms of activities. *Chem. Eng. Sci.* 62, 5753-5769.
- 429 Ho, Y.S., McKay, G., 1999. Pseudo-second order model for sorption processes. *Proc. Biochem.*
430 34, 451-465.
- 431 Huijgen, W.J.J., Witkamp, G.J., Comans, R.N.J., 2006. Mechanisms of aqueous wollastonite
432 carbonation as a possible CO₂ sequestration process. *Chem. Eng. Sci.* 61, 4242-4251.
- 433 IPCC (Intergovernmental Panel on Climate Change), 2007a. *Climate Change 2007: The Physical*
434 *Science Basis: Summary for Policymakers.* [http://ipcc-](http://ipcc-wg1.ucar.edu/wg1/Report/AR4WG1_Pub_SPM-v2.pdf)
435 [wg1.ucar.edu/wg1/Report/AR4WG1_Pub_SPM-v2.pdf](http://ipcc-wg1.ucar.edu/wg1/Report/AR4WG1_Pub_SPM-v2.pdf)
- 436 IPCC (Intergovernmental Panel on Climate Change), 2007b. *Climate Change 2007: Climate*
437 *Change Impacts, Adaptations, and Vulnerability.* <http://ipcc-wg2.org/index.html>
- 438 Juvekar, V.A., Sharma, M.M., 1973. Absorption of CO₂ in a suspension of lime. *Chem. Eng. Sci.*
439 28, 825-837.
- 440 Kaszuba, J.P., Janecky, D.R., Snow, M.G., 2003. Carbon dioxide reaction processes in a model
441 brine aquifer at 200 °C and 200 bars: implications for geologic sequestration of carbon.
442 *Appl. Geochem.* 18, 1065-1080.

- 443 Kaszuba, J.P., Janecky, D.R., Snow, M.G., 2005. Experimental evaluation of mixed fluid
444 reactions between supercritical carbon dioxide and NaCl brine: Relevance to the integrity of
445 a geologic carbon repository. *Chem. Geol.* 217, 277-293.
- 446 Kharaka, Y.K., Cole, D.R., Hovorka, S.D., Gunter, W.D., Knauss, K.G., Friefeld, B.M., 2006.
447 Gas-water-rock interactions in Frio Formation following CO₂ injection: Implications for the
448 storage of greenhouse gases in sedimentary basins. *Geology* 34, 577-580.
- 449 Kugge, C., Daicic, J., 2004. Shear response of concentrated calcium carbonate suspensions. *J.*
450 *Colloid Interface Sci.* 271, 241-248.
- 451 Lagergren, S., 1898. About the theory of so-called adsorption of soluble substances. *K. Sven.*
452 *Vetenskapsakad. Handlingar*, Band 24, 1-39.
- 453 Maroto-Valer, M.M., Fauth, D.J., Kuchta, M.E., Zhang, Y., Andrésen, J.M., 2005. Activation of
454 magnesium rich minerals as carbonation feedstock materials for CO₂ sequestration. *Fuel*
455 *Process. Technol.* 86, 1627-1645.
- 456 Montes-Hernandez, G., Pérez-López, R., Renard, F., Nieto, J.M., Charlet, L., 2007a. Mineral
457 sequestration of CO₂ by aqueous carbonation of coal combustion fly-ash. *J. Hazard. Mater.*,
458 submitted.
- 459 Montes-Hernandez, G., Renard, F., Geoffroy, N., Charlet, L., Pironon, J., 2007b. Calcite
460 precipitation from CO₂-H₂O-Ca(OH)₂ slurry under high pressure of CO₂. *J. Cryst. Growth*
461 308, 228-236.
- 462 Murray, C.N., Wilson, T.R.S., 1997. Marine carbonate formations: their role in mediating long-
463 term ocean-atmosphere carbon dioxide fluxes-a review. *Energy Conver. Manage.* 38, 287-
464 294.
- 465 Parkhurst, D.L., Appelo, C.A.J., 2005. PHREEQC-2 version 2.12: A hydrochemical transport
466 model. <http://wwwbrr.cr.usgs.gov>.

- 467 Rau, G.H., Knauss, K.G., Langer, W.H., Caldeira, K., 2007. Reducing energy-related CO₂
468 emissions using accelerated weathering of limestone. *Energy* 32, 1471-1477.
- 469 Rendek, E., Ducom, G., Germain, P., 2006. Carbon dioxide sequestration in municipal solid
470 waste incinerator (MSWI) bottom ash. *J. Hazard. Mater.* B128, 73-79.
- 471 Shih, S.M., Ho, C.S., Song, Y.S., Lin, J.P., 1999. Kinetics of the Reaction of Ca(OH)₂ with CO₂
472 at Low Temperature. *Ind. Eng. Chem. Res.* 38, 1316-1322.
- 473 Soong, Y., Fauth, D.L., Howard, B.H., Jones, J.R., Harrison, D.K., Goodman, A.L., Gray, M.L.,
474 Frommell, E.A., 2006. CO₂ sequestration with brine solution and fly ashes. *Energy*
475 *Convers. Manage.* 47, 1676-1685.
- 476

477 **Tables**

478

479 Table 1. Experimental conditions and results of CO₂ sequestration experiments using paper mill
480 waste. Saturation state of calcite was calculated simulating with PHREEQC the reaction between
481 Millipore MQ water (pH 5.6) and portlandite (8.69 g) for different initial conditions of
482 temperature and CO₂ pressure.

483

484

485 **Figure captions**

486

487 Figure 1. SEM image of paper mill waste before experimentation showing the initial crystals of
488 portlandite, calcite and hydroxyapatite.

489

490 Figure 2. Schematic experimental system for sequestration of CO₂ by aqueous carbonation of
491 paper mill waste in a continuously stirred reactor.

492

493 Figure 3. XRD patterns of starting paper mill waste and solid products after carbonation during 2
494 and 48 h. C: Calcite, P: Portlandite, H: Hydroxyapatite. These spectra demonstrate the total
495 consumption of portlandite and the production of calcite.

496

497 Figure 4. (a-b) SEM images of calcite particles precipitated during CO₂ sequestration
498 experiments.

499

500 Figure 5. (a) Linear correlation between the pressure drop and the initial pressure of CO₂ for
501 experiments at 30 °C, an initial pressure of CO₂ equal to 10, 20, 30 and 40 bar and 2 h of
502 carbonation. (b) Kinetic behaviour of the CO₂ pressure drop in the long-term experiment (48 h) at
503 30 °C and 30 bar of initial pressure of CO₂. In both, constant pressure drop of 2.5 bar is
504 independent on the initial pressure of CO₂, showing that the thermodynamic state of CO₂
505 (gaseous or supercritical) does not modify the kinetics of reaction.

506

507 Figure 6. Kinetic modelling of sequestered quantity of CO₂ in the long-term experiment (48 h) at
508 30 °C and 30 bar of initial pressure of CO₂.

Experiment	Reactor content	Duration (h)	Temp. (°C)	Initial CO ₂ pressure (bar)	Final CO ₂ pressure (bar)	CO ₂ pressure-drop (bar)	Carbonation pressure (bar)	SI _{calcite}
Experiment 1	Blanks*	2	30	40	30.5	9.5	-	-
	1L pure water + 20 g of paper waste	2	30	40	28	12	2.5	1.13
Experiment 2	Blanks*	2	30	30	22.5	7.5	-	-
	1L pure water + 20 g of paper waste	2	30	30	20	10	2.5	1.25
Experiment 3	Blanks*	2	30	20	15	5	-	-
	1L pure water + 20 g of paper waste	2	30	20	12.5	7.5	2.5	1.42
Experiment 4	Blanks*	2	30	10	7.5	2.5	-	-
	1L pure water + 20 g of paper waste	2	30	10	5.3	4.7	2.2	1.71
Experiment 5	Blanks*	48	30	30	21.5	8.5	-	-
	1L pure water + 20 g of paper waste	48	30	30	19	11	2.5	1.25
Experiment 6	Blanks*	2	60	30	24.5	5.5	-	-
	1L pure water + 20 g of paper waste	2	60	30	21.5	8.5	3	1.52

*Blanks include two experiments of dissolution-dissociation of CO₂: (1) into pure water and (2) into a solution containing 1 g L⁻¹ of Ca. Both experiments showed identical results.

Table 1

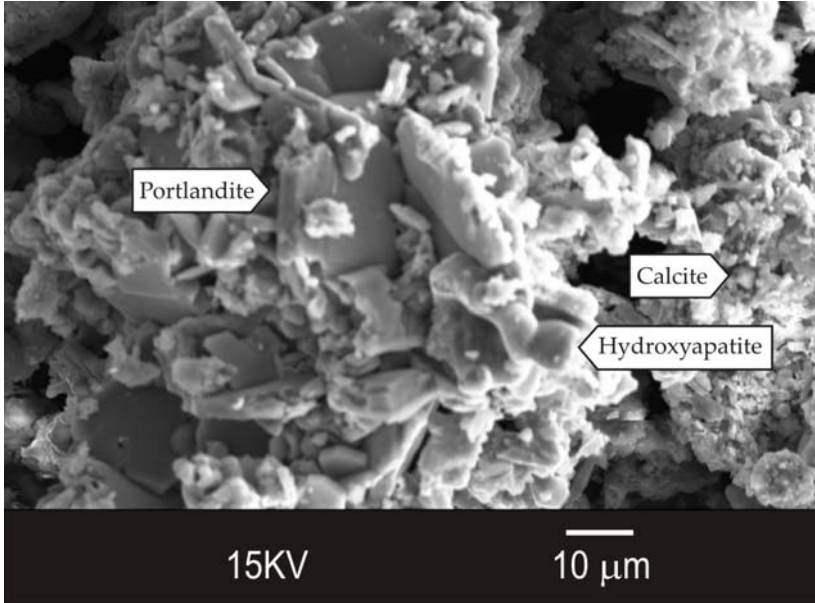


Figure 1

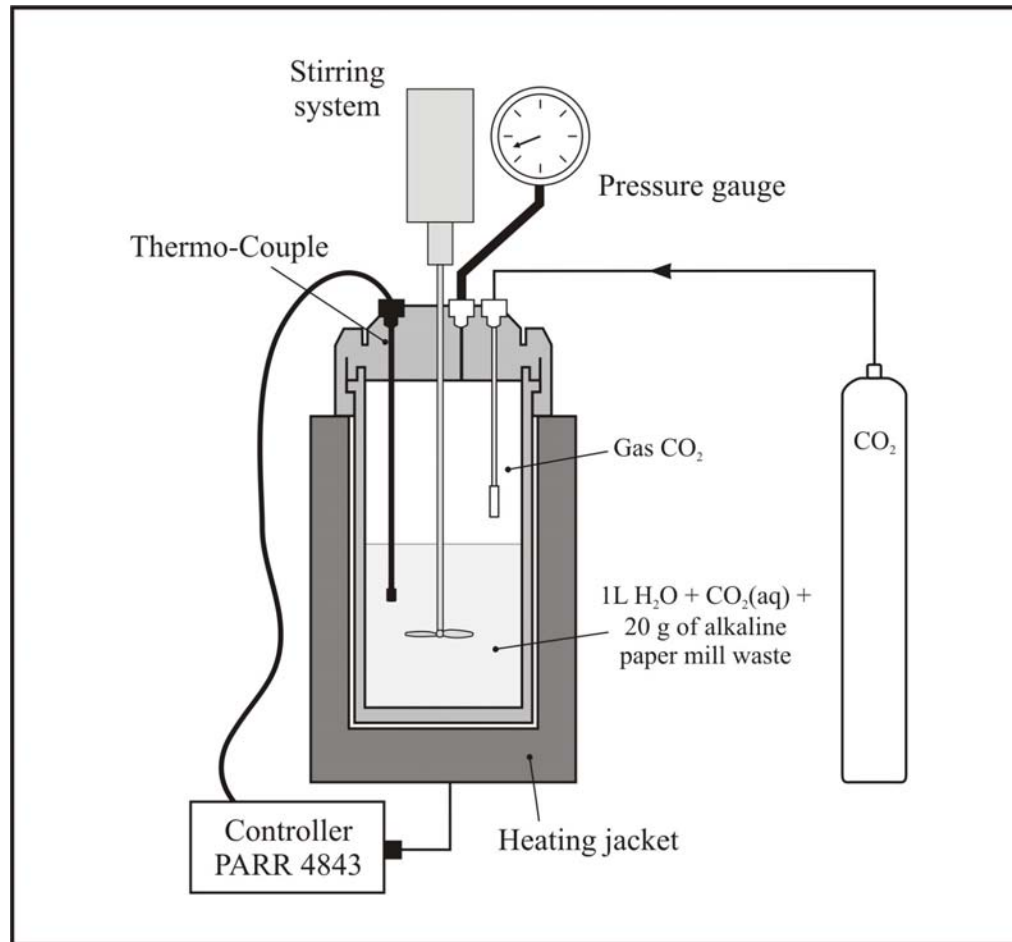


Figure 2

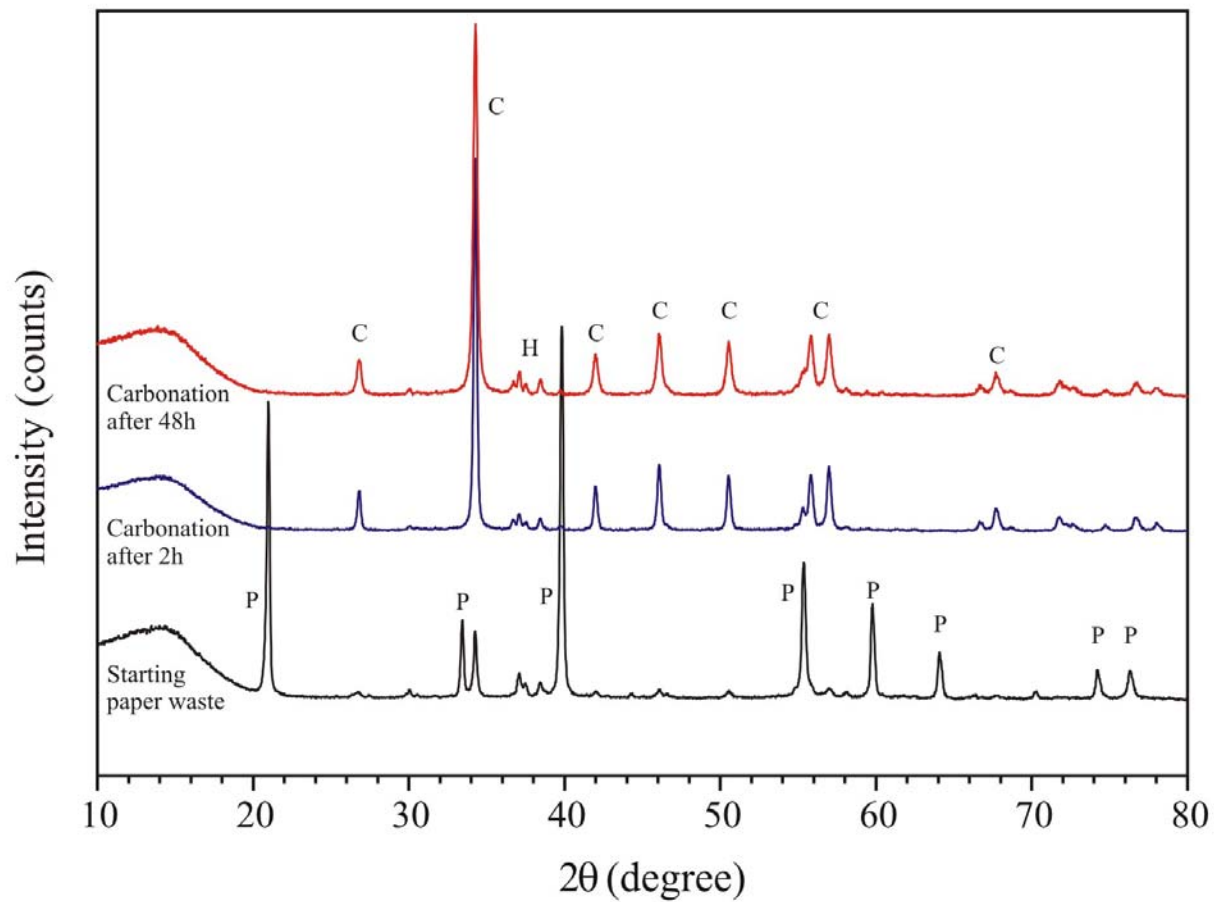


Figure 3

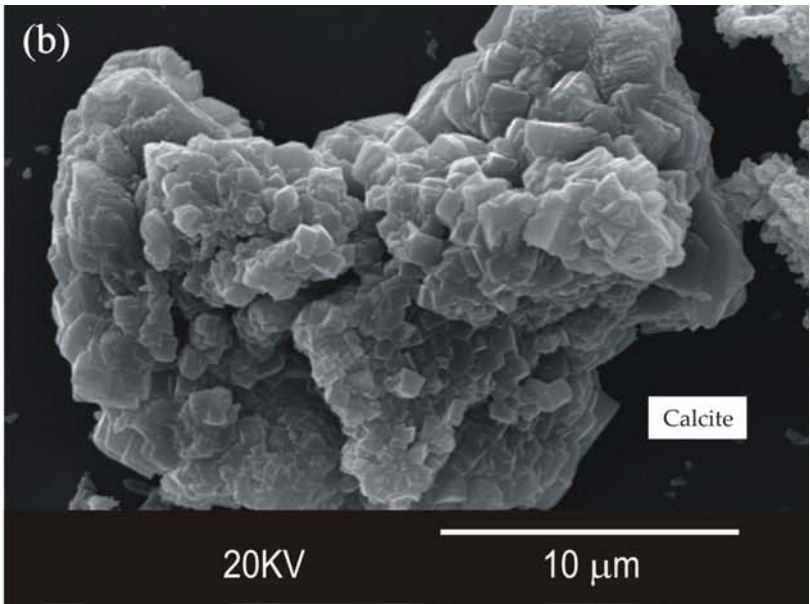
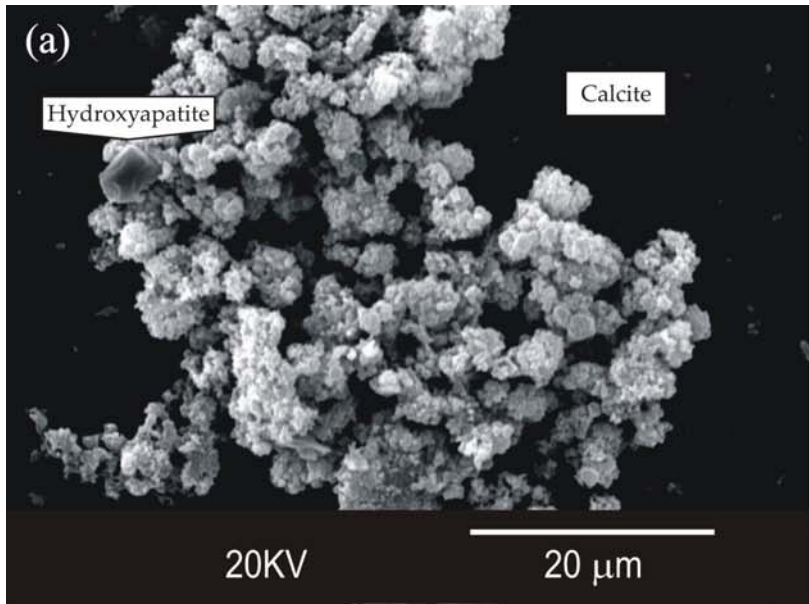


Figure 4

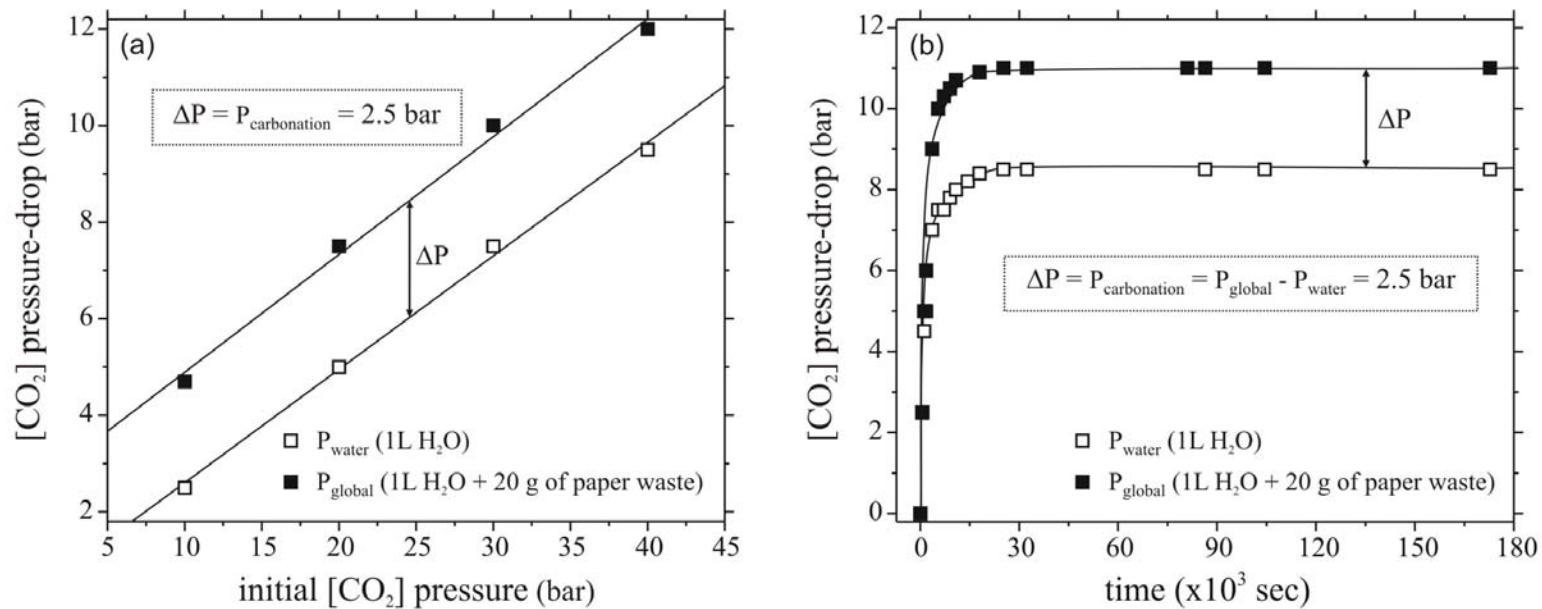


Figure 5

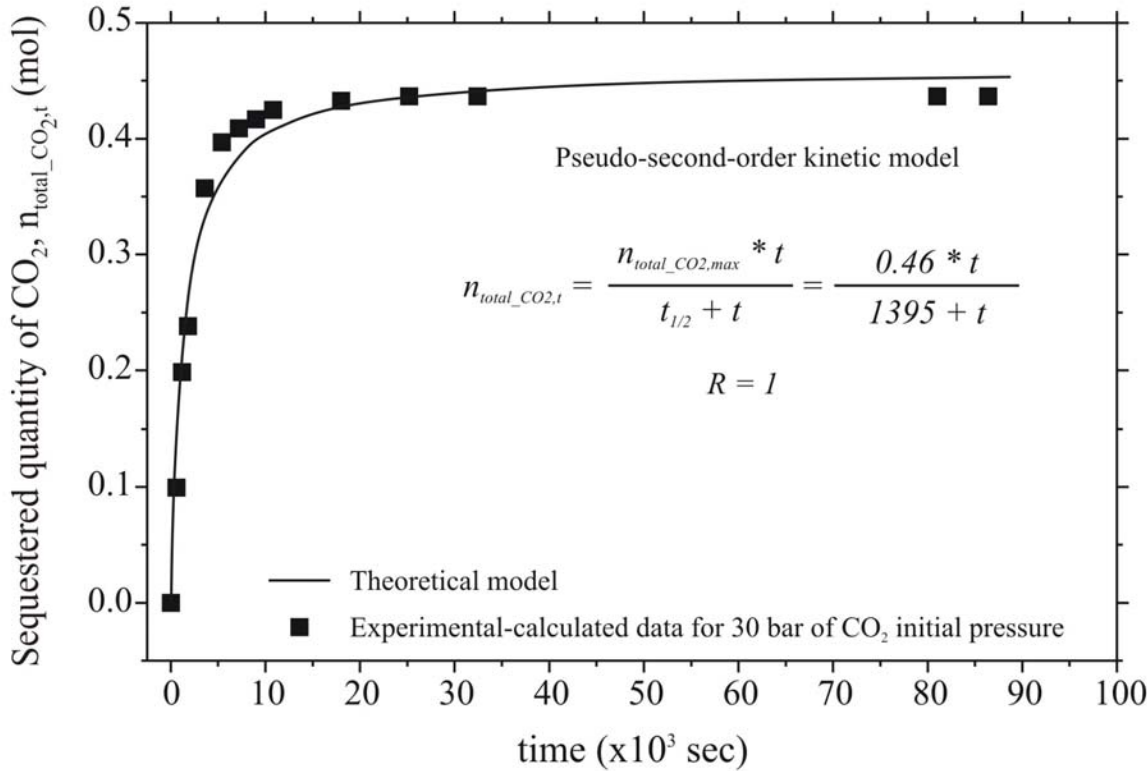


Figure 6